JCN Open Access ORIGINAL ARTICLE

pISSN 1738-6586 / eISSN 2005-5013 / J Clin Neurol 2022;18(5):581-593 / https://doi.org/10.3988/jcn.2022.18.5.581

Variations of Resting-State EEG-Based Functional Networks in Brain Maturation From Early Childhood to Adolescence

Yoon Gi Chung[a]
Yonghoon Jeon[a]
Ryeo Gyeong Kim[a]
Anna Cho[a]
Hunmin Kim[a]
Hee Hwang[a]
Jieun Choi[b]
Ki Joong Kim[c]

[a]Department of Pediatrics, Seoul National University Bundang Hospital, Seoul National University College of Medicine, Seongnam, Korea
[b]Department of Pediatrics, Seoul Metropolitan Government-Seoul National University Boramae Medical Center, Seoul, Korea
[c]Department of Pediatrics, Seoul National University Children's Hospital, Seoul National University College of Medicine, Seoul, Korea

Background and Purpose Alterations in human brain functional networks with maturation have been explored extensively in numerous electroencephalography (EEG) and functional magnetic resonance imaging studies. It is known that the age-related changes in the functional networks occurring prior to adulthood deviate from ordinary trajectories of network-based brain maturation across the adult lifespan.

Methods This study investigated the longitudinal evolution of resting-state EEG-based functional networks from early childhood to adolescence among 212 pediatric patients (age 12.2±3.5 years, range 4.4−17.9) in 6 frequency bands using 8 types of functional connectivity measures in the amplitude, frequency, and phase domains.

Results Electrophysiological aspects of network-based pediatric brain maturation were characterized by increases in both functional segregation and integration up to middle adolescence. EEG oscillations in the upper alpha band reflected the age-related increases in mean node strengths and mean clustering coefficients and a decrease in the characteristic path lengths better than did those in the other frequency bands, especially for the phase-domain functional connectivity. The frequency-band-specific age-related changes in the global network metrics were influenced more by volume-conduction effects than by the domain specificity of the functional connectivity measures.

Conclusions We believe that this is the first study to reveal EEG-based functional network properties during preadult brain maturation based on various functional connectivity measures. The findings potentially have clinical applications in the diagnosis and treatment of age-related brain disorders.

Keywords electroencephalography; rest state; functional connectivity; graph theory; child; brain maturation.

INTRODUCTION

The human brain comprises a network of spatially separated functional regions. Functional connectivity refers to the interregional statistical relationships of brain activities with region-to-region undirectional pairwise association matrices and connections.[1-3] Scalp electroencephalography (EEG) is a noninvasive method for recording neurophysiological activities in the human brain. EEG-based functional connectivity studies generally follow a series of analytical approaches: statistical estimation of region-to-region functional connectivity in multiple frequency bands; construction of association matrices representing the estimated functional connections to yield functional networks; and using graph-theory-based approaches to interpret the functional networks. Resting-state EEG-based functional networks are obtained by applying functional connectivity techniques to EEG recordings obtained in resting-state conditions in which participants remain awake and do not

Received November 3, 2021
Revised February 8, 2022
Accepted February 8, 2022

Correspondence
Hunmin Kim, MD, PhD
Division of Pediatric Neurology, Department of Pediatrics, Seoul National University Bundang Hospital, Seoul National University College of Medicine, 82 Gumi-ro 173 Beon-gil, Bundang-gu, Seongnam 13620, Korea
Tel +82-31-787-7289
Fax +82-31-787-4054
E-mail hunminkim@snubh.org

engage in cognitive or behavioral tasks.[1] Patterns of functional connectivity during the resting state have been suggested as network-based outcomes of intrinsic neural activities.[4]

Various methods have been proposed for estimating human brain functional connections, referred to as functional connectivity measures. These methods are based on different mathematical backgrounds depending on how the neurophysiological dynamics are interpreted, and so they may produce different outcomes.[5,6] For EEG-based functional connectivity, the measures are categorized into several groups based on the types of EEG properties exploited to estimate interregional functional connections, such as amplitude, frequency, phase, and uncertainty in information theory.[4,7,8] Each functional connectivity measure distinctly reflects its specific interregional interactions, and hence it is important to select appropriate metrics for handling EEG signals efficiently and to combining outcome generated by multiple functional connectivity measures in order to understand functional networks in a complementary manner.[9-13] Due to the inherent spatial dispersion of the electromagnetic fields during EEG recordings, spurious interactions induced by volume-conduction effects need to be discarded by using specific functional connectivity measures. A spurious interaction between two EEG signals from different regions will indicate the presence of a functional connection induced by the same electromagnetic source. It has been suggested that volume-conduction effects in EEG-based functional connectivity can be reduced by excluding or unmixing zero-lag components.[14,15]

Resting-state functional connectivity has been widely adopted to elucidate age-related network alterations during the brain maturation that occurs in the childhood, adolescence, and early adulthood periods that are associated with the continual refinement of neuronal connections and specialization of functional systems.[16-18] Many functional magnetic resonance imaging (fMRI) studies have found significant changes in the organization of resting-state functional networks in terms of segregation and integration that are associated with healthy aging from 7 to 31 years.[19-24] EEG studies have also found age-related changes in the resting-state functional networks from 5 to 7 years,[25,26] from 8 to 12 years,[27] and from infancy to 17 years,[28] in terms of variations in network characteristics such as strength, stability, segregation, and integration using a single functional connectivity measure. In particular, segregation of the resting-state functional networks increases from childhood to young adulthood, whereas it decreases throughout the adult lifespan from 20 years of age, implying different longitudinal trajectories of brain maturation over the human lifespan.[16] Therefore, a deeper understanding of brain maturation over different age periods is needed in fields such as pediatric neurology, cognitive neuroscience, and neurophysiology by performing wide explorations of age-related variations in functional networks. Achieving this requires a representative sample population that includes participants whose ages are distributed across childhood and adolescence. In addition, a single functional connectivity measure may be insufficient to elucidate the complicated age-related network-level variability, particularly for EEG-based functional networks. However, no resting-state EEG-based functional connectivity study has been conducted to reveal the network-based information in pre-adult brain maturation using various functional connectivity measures.

In this study, we aimed to characterize the longitudinal evolution of resting-state EEG-based functional networks from early childhood to adolescence. We constructed functional networks across ages in six frequency bands using eight types of functional connectivity measures belonging to the amplitude, frequency, and phase domains, with the following specific aims: 1) to clarify electrophysiological aspects of brain maturation during childhood and adolescence in terms of functional segregation and integration, 2) to identify the frequency band and functional connectivity measure that optimally reflect the age-related changes in functional network properties, and 3) to use various measures to reveal how the methodology affects frequency-band-specific age-related variations of functional network properties.

METHODS

Data set

This study was approved by the Institutional Review Board (IRB) of Seoul National University Bundang Hospital (IRB No. B-1807-478-107) and Seoul Metropolitan Government-Seoul National University Boramae Medical Center (IRB No. 20-2020-151). These IRBs waived the requirement to obtain informed consent due to the retrospective nature of the review of medical records and EEG data.

This study selected 212 pediatric patients in Seoul National University Bundang Hospital and Seoul Metropolitan Government-Seoul National University Boramae Medical Center aged 12.2±3.5 years (range 4.4−17.9), comprising 104 females aged 12.1±3.4 years and 108 males aged 12.3±3.6 years. The EEG records of patients who visited our pediatric neurology clinic for symptoms such as syncope or seizure-like events were included. Pediatric neurologists confirmed the presence of normal development based on patient histories and neurological examinations, and ruled out seizures based on patient symptoms in EEG examinations. The 212 patients were categorized into the following five age groups: 4−6 years (n=10; 3 females), 6−9 years (n=39; 21 females), 9−12 years (n=45; 24 females), 12−15 years (n=64; 30 females), and 15−18 years

(*n*=54; 26 females). The distribution of patients according to age and sex is shown in Fig. 1. EEG recordings were obtained using a 32-channel digital EEG system (Grass Telefactor, West Warwick, RI, USA) at a sampling frequency of 200 or 400 Hz while using a 60 Hz notch filter and 19 scalp electrodes according to the international 10–20 system. Waking and sleep EEG records were obtained whenever possible, and patients were sedated with chloral hydrate (50 mg/kg; maximum, 1 g) when necessary. All of the EEG recordings that were clinically interpreted as normal and seizure-free were selected, and the waking EEG records of relaxed wakefulness were checked by pediatric epileptologists (H.K. and H.H.) and they were re-referenced to average reference montages with 19 channels for subsequent processing. Down-sampling to 200 Hz was applied to the EEG recordings sampled at 400 Hz.

Estimation of functional connectivity

Artifact-free epochs (11.5±4.7 epochs) were extracted for each patient after visually inspecting for artifacts such as eye movements, muscle activities, and movements. The epoch length was set to 8 s not only to access the lowest frequency band but also to minimize instability in functional connectivity.[29] The following eight types of well-known functional connectivity measures were applied to the artifact-free epochs separately when estimating the interregional functional connections: correlation coefficient (CC)[7,30] and zero-lag-removed correlation coefficient (zCC)[30,31] as amplitude-domain measures; coherence (Coh) and the imaginary part of coherency (iCoh)[32] as frequency-domain measures; and phase-locking value (PLV),[15,33,34] phase-lag index (PLI),[35] weighted phase-lag index (wPLI),[36] and lagged phase synchronization (LPS)[37,38] as phase-domain measures. Among these eight measures, CC, Coh, and PLV are susceptible to volume-conduction effects, whereas the others are immune to such effects by excluding zero-lag components. The eight types of functional connectivity measures are described in detail in the Supplementary Material (in the online-only Data Supplement).

All epochs were band-pass filtered using sixth-order Butterworth filters into the following frequency bands: delta (0.5–4 Hz), theta (4–8 Hz), lower alpha (8–10 Hz), upper alpha (10–13 Hz), alpha (8–13 Hz), and beta (13–30 Hz). An association matrix for undirected weighted whole-brain functional connectivity with a size of 19×19 was constructed in each frequency band by each functional connectivity measure for each epoch, yielding a set of association matrices with a size of 19 channels×19 channels×6 bands×8 measures ×*m* for each patient, where *m* denotes the number of epochs. A representative association matrix for each patient was de-

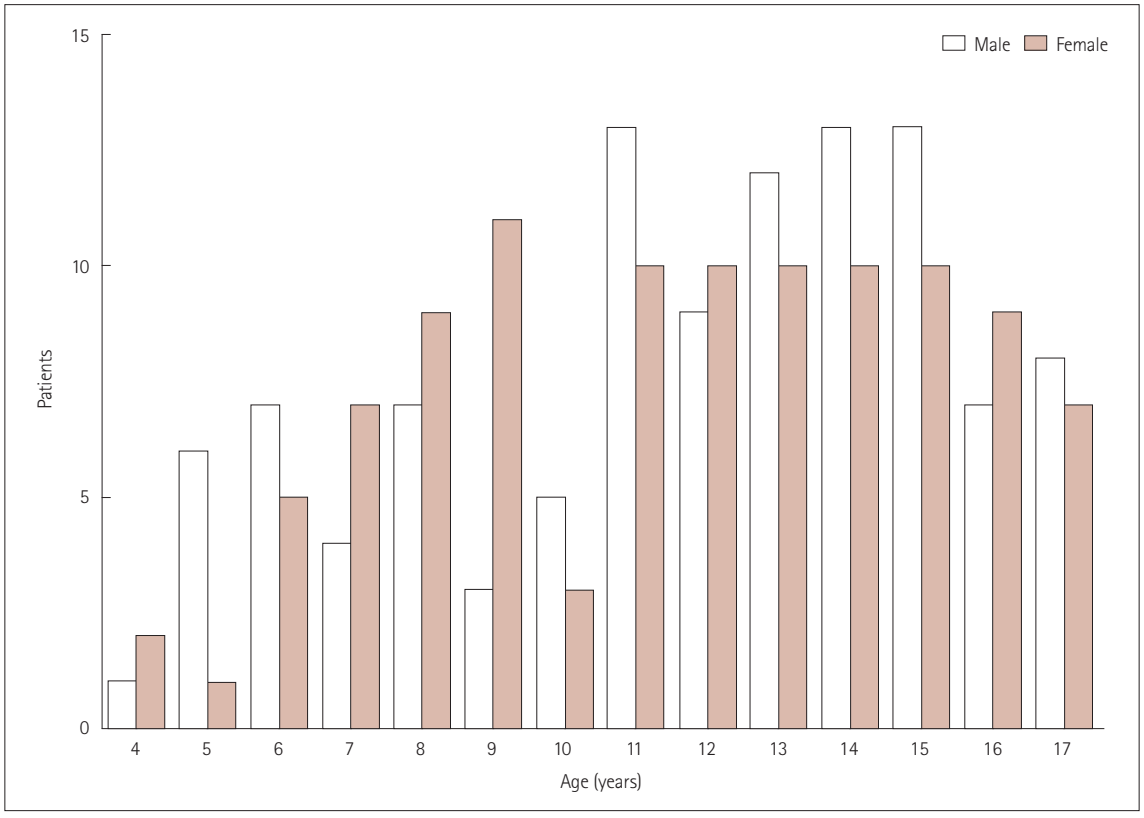

Fig. 1. A histogram of the number of patients by age and sex.

termined by averaging the set of association matrices over m epochs for each patient. The patient-level representative association matrices were used in subsequent graph-theory-based analyses. All of the association matrices were constructed using Python (version 3.6; Python Software Foundation, Wilmington, DE, USA) with the PyTorch library (version 1.4.0). Functional connectivity maps were generated across the five age groups by averaging the patient-level association matrices over patients in each age group, yielding five maps corresponding to each frequency band and each functional connectivity measure. Exemplar functional connectivity maps in the upper alpha band estimated using zCC, iCoh, PLV, and PLI are shown in Fig. 2. Detailed functional connectivity maps in the six frequency bands for the eight types of functional connectivity measures are shown in the Supplementary Material (Supplementary Figs. 1–6 in the online-only Data Supplement).

Analysis of functional network properties

When applying graph theory to EEG-based functional network analysis, nodes and edges correspond to EEG channels and interregional functional connections, respectively.[1,39] In the present study, each undirected weighted functional network had 19 nodes corresponding to 19 EEG channels and 171 edges corresponding to the pairwise undirected interregional functional connections. The weight of each edge represented the strength of the corresponding interregional functional connection. To quantify functional network properties, node strengths, clustering coefficients, and characteristic path lengths were selected as network metrics determined by the nodes and edges of the graph. The strength of a particular node quantifies the strength of functional connectivity at that node by taking the sum of weights of edges connected to it. The clustering coefficient quantifies the tendency of nodes to cluster together. Both the node strength and clustering coefficient are local network metrics that quantify functional network properties

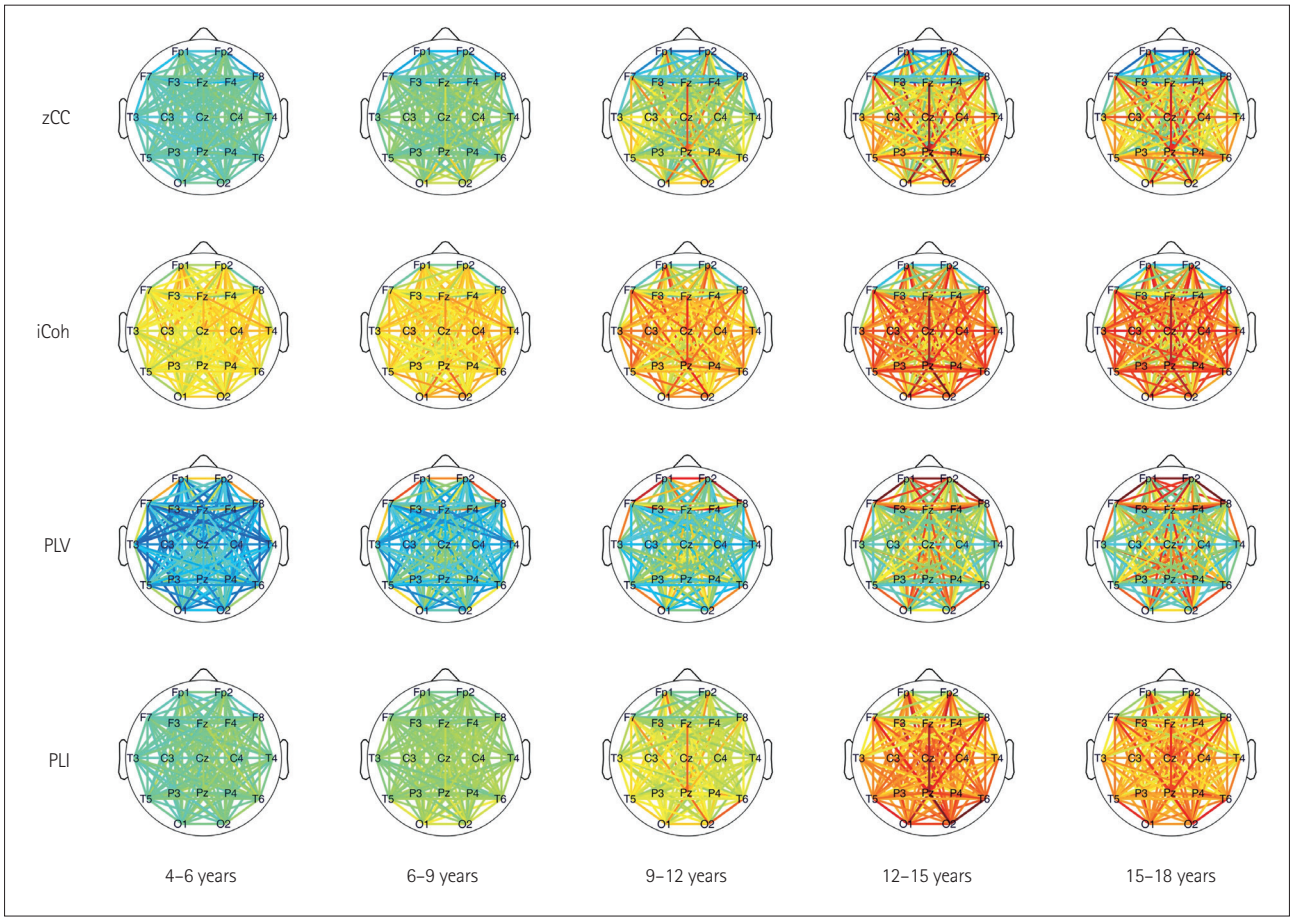

Fig. 2. Exemplar functional connectivity maps in the upper alpha band across five age groups estimated based on the 95% CIs of the zCC (0.00–0.54), iCoh (0.00–0.25), PLV (0.00–0.84), and PLI (0.00–0.30). Each map represents the functional connectivity averaged over patients in each age group. Maximum values of the strength of functional connectivity vary in accordance with the functional connectivity measures in order to improve the visualization. CI, confidence interval; iCoh, imaginary part of coherency; PLI, phase-lag index; PLV, phase-locking value; zCC, zero-lag-removed correlation coefficient.

at the node level. The mean node strength and the mean clustering coefficient reflect the overall strength of functional connectivity and the overall degree of segregation (or specialization) in a functional network, respectively, which are obtained by averaging the local network metrics over all nodes. The characteristic path length quantifies the degree of integration (whose inverse corresponds to efficiency) in a functional network, which is obtained by taking the mean shortest path length averaged over all pairs of nodes. The mean node strength, mean clustering coefficient, and characteristic path length are global network metrics that quantify functional network properties at the network level.[1,39]

In this study, 2 data matrices with a size of 212 patients×19 channels×6 bands×8 measures were obtained for the local network metrics: the node strength and the clustering coefficient. By averaging these local metrics over 19 channels, 2 data matrices with a size of 212 patients×6 bands×8 measures were obtained for the mean node strength and the mean clustering coefficient. An additional data matrix with a size of 212 patients×6 bands×8 measures was obtained for the characteristic path length. These three global network metrics were used in subsequent statistical analyses.

Statistical analyses

To estimate linear relationships between age groups and functional network properties, linear regression models with the first-order polynomials were applied to the global network metrics in the six frequency bands for the eight types of functional connectivity measures separately. The strength of the correlations were quantified as follows using the Pearson correlation coefficient (r): weak if $|r| < 0.4$, moderate if $|r| \geq 0.4$ and < 0.7, and strong if $|r| \geq 0.7$.[40] To compare means of the global network metrics between the five age groups, two-tailed two-sample t-tests assuming unknown and unequal variances were performed for all possible pairwise combinations of the age groups in the six frequency bands for the eight types of functional connectivity measures. The Benjamini-Yekutieli method[41] was applied to correct p values in multiple comparisons. Detailed information on the means of the global network metrics corresponding to each age group is presented in the Supplementary material (Supplementary Tables 1−3 in the online-only Data Supplement).

Calculation of the network metrics, visualization of the functional connectivity maps, and statistical analyses were performed using MATLAB (MathWorks, Natick, MA, USA) with the Brain Connectivity Toolbox (sites.google.com/site/bctnet) 39 and EEGLAB (sccn.ucsd.edu/eeglab).[42]

RESULTS

We investigated changes in functional network properties over the age range from 4.4 to 17.9 years based on the linear relationships between age and global network metrics. Detailed results from the linear regression models in the six frequency bands for the eight types of functional connectivity measures are presented in Table 1. We defined the age-related changes as significant if their linear regression models yielded p values less than 0.05, 95% confidence intervals (CIs) that did not include 0, and $|r|$ greater than or equal to 0.4.

Regarding the mean node strengths, CC, Coh, and PLV showed significant age-related increases in the delta (r=0.48 and CI=0.37−0.58, r=0.44 and CI=0.32−0.54, and r=0.47 and CI=0.35−0.57, respectively), upper alpha (r=0.72 and CI=0.64−0.78, r=0.73 and CI=0.66−0.79, and r=0.66 and CI=0.57−0.73, respectively), alpha (r=0.55 and CI=0.45−0.64, r=0.72 and CI=0.65−0.78, and r=0.45 and CI=0.34−0.55, respectively), and beta (r=0.75 and CI=0.68−0.80, r=0.71 and CI=0.63−0.77, and r=0.73 and CI=0.66−0.79, respectively) bands; while PLI, wPLI, and LPS showed significant age-related increases solely in the upper alpha band (r=0.44 and CI=0.32−0.54, r=0.45 and CI=0.34−0.55, and r=0.43 and CI=0.31−0.53, respectively).

Regarding the mean clustering coefficients, CC, Coh, and PLV showed significant age-related increases in the delta (r=0.45 and CI=0.34−0.55, r=0.41 and CI=0.29−0.51, and r=0.43 and CI=0.31−0.53, respectively), upper alpha (r=0.70 and CI=0.62−0.76, r=0.72 and CI=0.65−0.78, and r=0.66 and CI=0.57−0.73, respectively), alpha (r=0.54 and CI=0.44−0.63, r=0.72 and CI=0.65−0.78, and r=0.47 and CI=0.35−0.56, respectively), and beta (r=0.74 and CI=0.67−0.80, r=0.71 and CI=0.63−0.77, and r=0.73 and CI=0.66−0.78, respectively) bands; while PLI, wPLI, and LPS showed significant age-related increases solely in the upper alpha band (r=0.45 and CI=0.34−0.55, r=0.46 and CI=0.35−0.56, and r=0.44 and CI=0.33−0.55, respectively), and zCC showed a significant age-related increase in the upper alpha band (r=0.41, CI=0.29−0.52).

Regarding the characteristic path lengths, CC, Coh, and PLV showed significant age-related decreases in the delta (r=-0.49 and CI=-0.59 to -0.38, r=-0.46 and CI=-0.56 to -0.35, and r=-0.50 and CI=-0.60 to -0.39, respectively), upper alpha (r=-0.78 and CI=-0.83 to -0.72, r=-0.77 and CI=-0.82 to -0.71, and r=-0.72 and CI=-0.78 to -0.65, respectively), alpha (r=-0.62 and CI=-0.70 to -0.53, r=-0.72 and CI=-0.78 to -0.65, and r=-0.50 and CI=-0.59 to -0.39), and beta (r=-0.77 and CI=-0.82 to -0.70, r=-0.68 and CI=-0.75 to -0.61, and r=-0.74 and CI=-0.80 to -0.68, respectively) bands; while PLI, wPLI, and LPS showed significant age-related decreases solely in the upper alpha band (r=-0.45 and CI=-0.55 to -0.33, r=-0.48

Table 1. Age-related changes in the global network metrics in the six frequency bands based on the eight types of functional connectivity measures

	CC	zCC	Coh	iCoh	PLV	PLI	wPLI	LPS
Mean node strength								
δ	0.48 [0.37, 0.58]	-0.39 [-0.50, -0.27]	0.44 [0.32, 0.54]	-0.15 [-0.28, -0.02]	0.47 [0.35, 0.57]	0.27 [0.14, 0.39]	0.29 [0.16, 0.41]	0.19 [0.05, 0.31]
θ	0.24 [0.11, 0.36]	-0.24 [-0.37, -0.11]	0.19 [0.05, 0.31]	-0.30 [-0.42, -0.18]	0.15 [0.02, 0.28]	-0.16 [-0.28, -0.02]	-0.13 [-0.26, 0.01]	-0.21 [-0.34, -0.08]
α (lower)	0.31 [0.18, 0.43]	-0.08 [-0.22, 0.05]	0.23 [0.10, 0.35]	-0.10 [-0.23, 0.04]	0.16 [0.03, 0.29]	-0.05 [-0.19, 0.08]	-0.05 [-0.18, 0.08]	-0.04 [-0.18, 0.09]
α (upper)	0.72 [0.64, 0.78]	0.38 [0.25, 0.49]	0.73 [0.66, 0.79]	0.29 [0.16, 0.41]	0.66 [0.57, 0.73]	0.44 [0.32, 0.54]	0.45 [0.34, 0.55]	0.43 [0.31, 0.53]
α	0.55 [0.45, 0.64]	0.12 [-0.02, 0.25]	0.72 [0.65, 0.78]	0.16 [0.02, 0.29]	0.45 [0.34, 0.55]	0.19 [0.06, 0.32]	0.21 [0.08, 0.33]	0.20 [0.07, 0.33]
β	0.75 [0.68, 0.80]	0.06 [-0.07, 0.20]	0.71 [0.63, 0.77]	-0.20 [-0.33, -0.07]	0.73 [0.66, 0.79]	0.02 [-0.12, 0.15]	0.08 [-0.06, 0.21]	0.21 [0.07, 0.33]
Mean clustering coefficient								
δ	0.45 [0.34, 0.55]	-0.36 [-0.47, -0.23]	0.41 [0.29, 0.51]	-0.12 [-0.25, 0.02]	0.43 [0.31, 0.53]	0.30 [0.17, 0.41]	0.32 [0.19, 0.44]	0.22 [0.09, 0.35]
θ	0.14 [0.01, 0.27]	-0.23 [-0.35, -0.10]	0.13 [0.00, 0.26]	-0.30 [-0.41, -0.17]	0.07 [-0.06, 0.21]	-0.14 [-0.27, -0.01]	-0.12 [-0.26, 0.01]	-0.18 [-0.30, -0.04]
α (lower)	0.29 [0.16, 0.41]	-0.10 [-0.24, 0.03]	0.23 [0.09, 0.35]	-0.12 [-0.25, 0.02]	0.17 [0.03, 0.30]	-0.07 [-0.20, 0.07]	-0.06 [-0.20, 0.07]	-0.07 [-0.20, 0.07]
α (upper)	0.70 [0.62, 0.76]	0.41 [0.29, 0.52]	0.72 [0.65, 0.78]	0.34 [0.22, 0.46]	0.66 [0.57, 0.73]	0.45 [0.34, 0.55]	0.46 [0.35, 0.56]	0.44 [0.33, 0.55]
α	0.54 [0.44, 0.63]	0.12 [-0.02, 0.25]	0.72 [0.65, 0.78]	0.20 [0.07, 0.33]	0.47 [0.35, 0.56]	0.19 [0.05, 0.31]	0.20 [0.07, 0.32]	0.18 [0.05, 0.31]
β	0.74 [0.67, 0.80]	0.09 [-0.05, 0.22]	0.71 [0.63, 0.77]	-0.19 [-0.32, -0.06]	0.73 [0.66, 0.78]	0.03 [-0.10, 0.17]	0.08 [-0.06, 0.21]	0.25 [0.12, 0.37]
Characteristic path length								
δ	-0.49 [-0.59, -0.38]	0.46 [0.35, 0.56]	-0.46 [-0.56, -0.35]	0.18 [0.05, 0.31]	-0.50 [-0.60, -0.39]	-0.22 [-0.34, -0.08]	-0.26 [-0.38, -0.13]	-0.14 [-0.27, 0.00]
θ	-0.34 [-0.45, -0.21]	0.34 [0.22, 0.46]	-0.24 [-0.36, -0.11]	0.35 [0.23, 0.46]	-0.27 [-0.39, -0.14]	0.16 [0.02, 0.28]	0.13 [-0.01, 0.26]	0.28 [0.15, 0.40]
α (lower)	-0.35 [-0.46, -0.23]	0.19 [0.06, 0.32]	-0.24 [-0.36, -0.10]	0.18 [0.04, 0.30]	-0.17 [-0.29, -0.03]	0.17 [0.03, 0.29]	0.14 [0.00, 0.27]	0.17 [0.03, 0.30]
α (upper)	-0.78 [-0.83, -0.72]	-0.39 [-0.50, -0.27]	-0.77 [-0.82, -0.71]	-0.31 [-0.42, -0.18]	-0.72 [-0.78, -0.65]	-0.45 [-0.55, -0.33]	-0.48 [-0.58, -0.37]	-0.44 [-0.54, -0.32]
α	-0.62 [-0.70, -0.53]	-0.07 [-0.20, 0.07]	-0.72 [-0.78, -0.65]	-0.19 [-0.32, -0.06]	-0.50 [-0.59, -0.39]	-0.14 [-0.27, -0.01]	-0.18 [-0.31, -0.05]	-0.16 [-0.28, -0.02]
β	-0.77 [-0.82, -0.70]	-0.03 [-0.16, 0.10]	-0.68 [-0.75, -0.61]	0.22 [0.09, 0.35]	-0.74 [-0.80, -0.68]	-0.03 [-0.16, 0.10]	-0.09 [-0.23, 0.04]	-0.13 [-0.26, 0.01]

Pearson correlation coefficients (r) and their 95% CIs denoted as [lower, upper] in linear regression models with the first-order polynomials are presented for the mean node strengths, mean clustering coefficients, and characteristic path lengths. Boldface indicates $p<0.05$, CI not including 0, and $|r| \geq 0.4$.

CC, correlation coefficient; CI, confidence interval; Coh, coherence; iCoh, imaginary part of coherency; LPS, lagged phase synchronization; PLI, phase-lag index; PLV, phase-locking value; wPLI, weighted phase-lag index; zCC, zero-lag-removed correlation coefficient.

and CI=-0.58 to -0.37, and r=-0.44 and CI=-0.54 to -0.32, respectively), and zCC showed a significant age-related increase in the delta band (r=0.46, CI=0.35–0.56).

Age-related changes in the mean node strengths, mean clustering coefficients, and characteristic path lengths in the upper alpha band based on the 8 types of functional connectivity measures of the 212 patients are shown in Fig. 3. The age-related changes in all six frequency bands are shown in detail in the Supplementary Material (Supplementary Figs. 7–9 in the online-only Data Supplement). No statistically significant change in the global network metrics was observed in the theta and lower alpha bands.

We examined differences between the means of global network metrics in the five age groups using two-tailed, two-sample t-tests for all possible pairwise combinations with p values corrected using the Benjamini-Yekutieli method. Differences were investigated especially closely in the upper alpha band because significant age-related changes in the global network metrics were predominant in that frequency band, as shown in Fig. 4.

Regarding the mean node strengths, all of the functional connectivity measures differed significantly between the age-group pairs of 4–6 years vs. 6–9 years, 6–9 years vs. 9–12 years, and 9–12 years vs. 12–15 years (p<0.05), except for zCC (4–6 years vs. 6–9 years, 6–9 years vs. 12–15 years, and 9–12 years vs. 12–15 years; p<0.05) and iCoh (4–6 years vs 9–12 years and 6–9 years vs. 12–15 years, p<0.05). Regarding the mean clustering coefficients, all of the functional connectivity measures differed significantly between the age-group pairs of 4–6 years vs. 6–9 years, 6–9 years vs. 9–12 years, and 9–12 years vs. 12–15 years (p<0.05), except for zCC and iCoh (4–6 years vs. 6–9 years, 6–9 years vs. 12–15 years, and 9–12 years vs. 12–15 years; p<0.05). Regarding the characteristic path lengths, CC, Coh, PLV, PLI, and wPLI differed significantly between the age-group pairs of 4–6 years vs. 6–9 years, 6–9 years vs. 9–12 years, and 9–12 years vs. 12–15 years (p<0.05), while zCC and iCoh differed between the age-group pairs of 4–6 years vs. 9–12 years, 6–9 years vs. 12–15 years, and 9–12 years vs. 12–15 years (p<0.05), and LPS differed between the age-group pairs of 4–6 years vs. 6–9 years, 6–9 vs. 12–15 years, and 9–12 years vs. 12–15 years (p<0.05). No statistically significant difference was observed between the age groups of 12–15 and 15–18 years for any of the global network metrics.

DISCUSSION

The three main findings of this resting-state EEG-based functional connectivity study are as follows:

1) Electrophysiological aspects of network-based pediat-

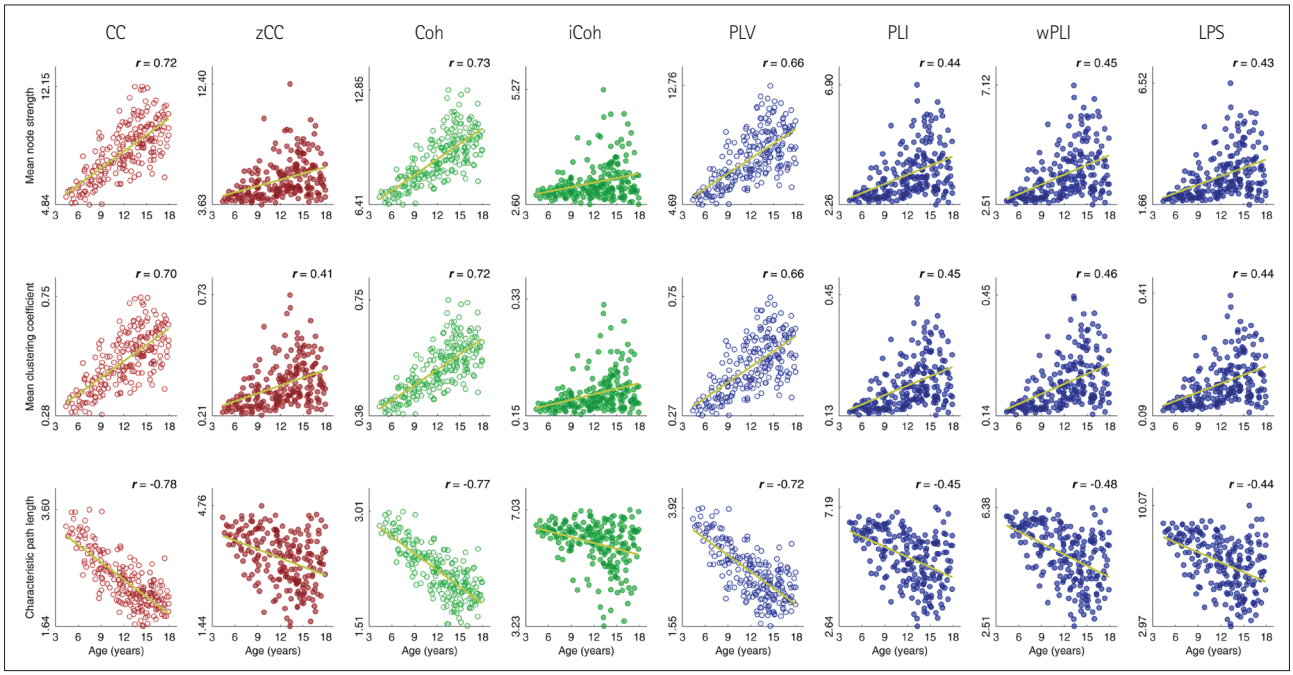

Fig. 3. Age-related changes in the global network metrics in the upper alpha band based on the eight types of functional connectivity measures. Pearson correlation coefficients (r) for linear regression models with first-order polynomials are shown if p<0.05, 95% CIs did not include 0, and $|r|$ ≥0.4. Yellow lines represent the first-order-polynomial trend lines. Y-axes vary according to the functional connectivity measures and global network metrics. CC, correlation coefficient; CI, confidence interval; Coh, coherence; iCoh, imaginary part of coherency; LPS, lagged phase synchronization; PLI, phase-lag index; PLV, phase-locking value; wPLI, weighted phase-lag index; zCC, zero-lag-removed correlation coefficient.

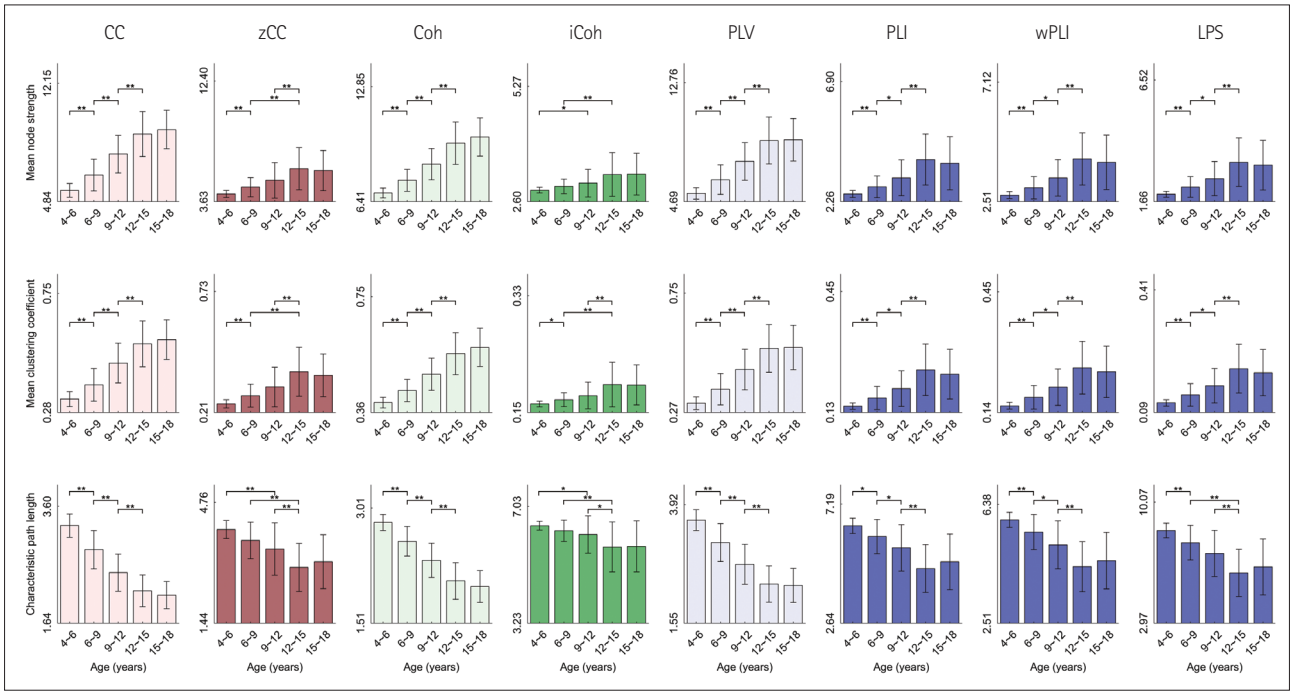

Fig. 4. Differences between the means of global network metrics for age groups in the upper alpha band based on the eight types of functional connectivity measures. Each bar represents a global network metric averaged over the patients in each age group. Horizontal lines at the top and bottom of each bar indicates the standard deviation (two-tailed two-sample t-tests between two age groups assuming unknown and unequal variances; *if $p<0.05$ and **if $p<0.01$; Benjamini-Yekutieli method for p-value correction). Y-axes vary according to the functional connectivity measures and global network metrics. CC, correlation coefficient; Coh, coherence; iCoh, imaginary part of coherency; LPS, lagged phase synchronization; PLI, phase-lag index; PLV, phase-locking value; wPLI, weighted phase-lag index; zCC, zero-lag-removed correlation coefficient.

ric brain maturation are characterized by noticeable increases in both functional segregation and integration up to middle adolescence.

2) EEG oscillations in the upper alpha band reflect longitudinal variations of functional network properties from early childhood to adolescence better than do those in other frequency bands, especially for the estimation of functional connectivity by phase-domain measures.

3) Volume-conduction effects have a greater influence on the frequency-band-specific age-related changes in functional network properties than does the domain specificity of the functional connectivity measure.

Functional segregation and integration during brain maturation

The present results indicate that the mean clustering coefficients increase and characteristic path lengths decrease with aging, particularly in the upper alpha band for phase-domain measures. This implies that the resting-state EEG-based functional networks in the healthy human brain show significant increases in the degree of segregation and integration from early childhood to adolescence. We therefore speculate that normal brain maturation during childhood and adolescence is characterized by functional specialization and efficiency enhancement. The characteristics of brain maturation across the healthy human lifespan revealed by many resting-state functional connectivity studies (particularly from early childhood to young adulthood) are at least partially consistent with our results. It may be challenging to directly compare our findings with those of previous studies due to variations in the technological approaches, such as EEG and fMRI, and demographic differences.

A recent EEG study found that, from 5 to 7 years, the synchronization likelihood-based functional connectivity decreased in the 4–6, 6–11, and 11–25 Hz bands, normalized clustering coefficients increased in the alpha band, and normalized characteristic path lengths increased in all frequency bands.[26] That study indicated that the age-related decrease in the strength of functional connectivity implied pruning of unused neuronal connections and retention of frequently used connections, thereby establishing cost-effective organized functional networks. Another EEG study found that the synchronization likelihood-based functional connectivity increased between the age groups of 5–7 and 16–18 years in the 6–13 and 15–25 Hz bands, accompanied by increases in the clustering coefficients and characteristic path lengths.[43] Unlike our approaches, those studies estimated the resting-state functional connectivity based on the pattern similarity

of EEG time series, their alpha band included both lower and upper alpha bands, and their age-related changes were observed solely within a narrow age range, in contrast with our findings. Coh-based interhemispheric functional connectivity increased from 8 to 12 years in the 1.5–3.5, 3.5–7.5, and 7.5–12.5 Hz bands, and was possibly related to an increase in the velocity of neural transmission resulting from myelination.[27] Phase shift durations approaching chaotic states increased from 2 months to 16 years, and were related to increases in functional stability and integration.[28] A recent fMRI study revealed age-related strengthening of the functional connectivity from 3 to 22 years, based on the finding that older participants tended to spend more time in each functional state.[44]

Age-related functional network reorganizations in terms of segregation and integration have been revealed in more detail by fMRI studies. The resting-state functional connectivity within brain systems decreases whereas the connectivity between brain systems increases with aging across the lifespan from 20 years of age in healthy adults.[16] However, there are deviations in the age-related variations during childhood and adolescence, indicating more-complex patterns of the network alterations, such as an increase in the functional connectivity within a certain brain system to establish functionally segregated areas.[16,21] For example, another fMRI study found that short-range functional connectivity was stronger in children aged 7–9 years than in adults aged 19–31 years, whereas long-range functional connectivity was stronger in adults than children.[19,24] The weakened short-range functional connectivity was interpreted as indicating the presence of selective pruning of synaptic connections, with the strengthened long-range functional connectivity associated with enhancement of neuronal signal transduction between distal regions by the addition of myelin sheaths. Other fMRI studies found that functional connections between default regions were denser during young adulthood (21–31 years) than early school age (7–9 years)[20]; that children and adolescents aged 8–17 years had local functional connectivity with short-distance interregional connections, while young adults aged 19–24 years had intermediate functional connectivity with long-distance connections;[22] that global interhemispheric functional connectivity between corresponding regions in each hemisphere decreased from childhood to adolescence (at 7–18 years) to reciprocally increase hemispheric specialization of cognitive functions;[45,46] and that weakening of local functional connectivity occurred in parallel with the setting up of long-range functional connectivity from late childhood to early adulthood (11–35 years),[47] supporting age-related increases in both functional segregation and integration.

We observed significant changes in the means of global network metrics of age groups from 4–6 to 12–15 years, but not from 12–15 to 15–18 years. A recent fMRI study identified a two-stage trajectory of brain development from 10 to 26 years, with functional networks stabilizing up to early adolescence (13–15 years) and then subsequently exhibiting increased integration through adulthood,[23] which conflicts with our findings and those of other studies mentioned above. However, another recent fMRI study that included subcortical regions found that the amygdala-cortical functional connectivity changed meaningfully at the transition from childhood to adolescence (i.e., at 10–11 years).[48] Hence, we cautiously suggest that electrophysiological aspects of network-based brain maturation are characterized by noticeable increases in both functional segregation and integration, and that other types of network-based brain maturation beyond the corticocortical functional connectivity can begin from middle adolescence. In terms of regional effects, some fMRI studies have found that the strength of functional connectivity increases with aging (from 7 to 31 years) between regions in the cinguloopercular network such as the dorsal anterior cingulate cortex, anterior insula, and frontal operculum,[19] as well as in the default network such as the medial prefrontal cortex, posterior cingulate cortex, and retrosplenial cortex.[20] However, some unclear aspects remain to be elucidated in future studies involving EEG, fMRI, and other brain imaging techniques in order to obtain a deeper understanding of brain maturation from early childhood to adolescence.

Age-related changes in the upper alpha band with phase-domain measures

Significant age-related changes in functional network properties were observed predominantly in the upper alpha band. In particular, all four phase-domain measures (PLV, PLI, wPLI, and LPS) showed significant age-related changes in all of the global network metrics in the upper alpha band. Considering the functional connectivity measures that are immune to volume-conduction effects, the r values for zCC and iCoh were higher in the upper alpha band than in the other frequency bands. However, their correlations in the upper alpha band were distinctly weaker than those of phase-domain measures.

Human physiological aging affects alpha-band EEG oscillations over the entire lifespan.[49-51] The aging process modulates healthy functional networks particularly in the upper alpha band.[49] A previous EEG study revealed the following age-related variations in the power in the upper alpha band: increasing from early childhood to adulthood, higher in 12-year-old children than in younger children, and higher following brain maturation at 16 years or older.[52] EEG oscillations in the upper alpha band reflect semantic memory processing related to knowledge acquisition, whereas those in the lower alpha band reflect attentional processing related to mental prep-

aration.[49,52] Furthermore, knowledge acquisition begins very early in childhood while semantic memory evolves during the preschool years.[53] Therefore, observations of distinct age-related changes in the global network metrics in the upper alpha band may be related to brain development associated with knowledge acquisition.

Delta-band EEG oscillations are related to physiological aging in adults[50] but not commonly in children under 18 years. A previous EEG study demonstrated age-related increases in the intra- and interhemispheric coherence both in the delta and alpha bands from 8 to 12 years, locally rather than globally.[27] Theta-band EEG oscillations are reportedly related to declines in neurocognitive functions in healthy elderly subjects.[49] It is presumed that only weak or nonsignificant theta-band age-related changes were induced in the global network metrics of healthy patients in the present study. Age-dependent characteristics of beta-band EEG oscillations have not been commonly reported; instead, they are affected by movements rather than by neurocognitive functions.[49] In particular, muscle artifacts during EEG recordings are more common in younger children than in adolescents and adults, and so the former might have high beta-band activity unrelated to aging. Regarding the age-related changes in the global network metrics in the delta, theta, lower alpha, and beta bands showing different patterns for eight measures (Table 1), further studies are required to clarify the potential effects of local network metrics on global ones due to regional variations in the age dependency.[27,54]

Directly comparing functional connectivity measures was beyond the scope of this study. In addition, each functional connectivity measure has its own characteristic advantages and disadvantages for estimating interregional functional connectivity. This means that it might not be straightforward to conclude that phase-domain measures are optimal for exploring age-related changes in functional network properties. However, age-related changes in the global network metrics in the upper alpha band are revealed in the functional networks estimated using the phase-domain measures more distinctly and consistently than when using the amplitude- and frequency-domain measures. We conjecture that phase-domain measures have some methodological benefits in separating amplitude effects from phase dynamics of EEG signals,[33,38] reducing amplitude variations of EEG oscillations,[55] and not requiring an assumption of stationarity.[33] Furthermore, interregional couplings identified by phase-domain measures are less related to structural networks and show stronger state dependency than those found by amplitude-domain measures.[56] Coh statistics can easily reject the null hypothesis of interregional couplings manifesting as white-noise signals.[33] Moreover, phase-domain measures are better for understanding interregional couplings within a specific frequency band, because frequency-domain measures estimate functional connectivity across a relatively wide frequency range. We therefore suggest that the changes in functional network properties with aging are more accurately reflected by EEG oscillations in the upper alpha band than by those in other frequency bands, and that phase-domain measures more accurately reflect age-related changes in functional network properties than do amplitude- and frequency-domain measures.

Volume-conduction effects on the age-related changes

Functional connectivity measures that are susceptible to volume-conduction effects showed noticeable frequency-band-specific age-related changes in functional network properties. CC, Coh, and PLV showed significant age-related changes in the global network metrics in the delta, upper alpha, alpha, and beta bands, regardless of their domain specificities. Some recent studies have identified unique roles of different types of functional connectivity measures. For example, CC and Coh were found to be suitable for stationary signals, whereas phase-based measures were suitable for nonstationary signals in detecting true connections in simulated EEG data sets.[9] Significant differences were identified between normal synchronization and epileptic synchronization when using nonlinear measures such as phase-based ones in the gamma band, and when using linear measures such as Coh in the lower frequency bands.[57] wPLI had high sensitivity for a mixture of linear and nonlinear interregional couplings in both simulated and real EEG data sets.[11] Since the present study adopted undirected functional connectivity measures, comparisons between undirected and directed[58] or between multiple directed functional connectivity measures[59] may have been beyond the scope of our study.

According to previous studies, the frequency-band-specific age-related changes in functional network properties were anticipated to be domain specific; that is, the amplitude-domain measures of CC and zCC showed similar changes, as did other measures in the frequency and phase domains. However, CC, Coh, and PLV showed similar changes despite them belonging to the amplitude, frequency, and phase domains, respectively. Since Coh and iCoh reflect amplitudes of EEG signals at a given frequency and are calculated based on interregional couplings independently for each frequency,[34] we categorized them as frequency-domain measures. The similarity of the changes might be attributable to the domain specificity being too subtle to be recognized in the functional networks. A previous study found that Coh and PLV provided essentially the same information on the coupling between healthy EEG signals during sleep.[60] Another reason

may be the strength of interregional functional connections being inflated by spurious or ghost connections, particularly in functional networks that are susceptible to volume-conduction effects.[15] In this regard, a recent EEG study found that both Coh and PLV overestimated functional connectivity, leading to greater strength than other measures when using simulated EEG signals.[61] Assuming that distinct volume-conduction effects exist, it is possible that CC, Coh, and PLV yield similar information about functional network properties. For these reasons, we suggest that frequency-band-specific age-related changes in functional network properties can be influenced more by volume-conduction effects than by the domain specificity of functional connectivity measures.

Limitations and further work

Our study was subject to several limitations. In terms of clinical limitations, we made every attempt to include neurologically intact healthy children, in order to represent normal brain maturation by analyzing the EEG records of patients who had no known brain disorder or pathology. However, functional study results were not available to confirm the presence normal cognitive functioning. In terms of technical limitations, we excluded certain types of functional connectivity measures based on information theory and amplitude-envelope correlation; we investigated global aspects of age-related changes in functional network properties rather than local aspects. The inclusion of a larger number of participants would have improved the ability to generalize our findings. For the future, we plan to enroll healthy children, perform cognitive function tests, add functional network measures not used in this study, explore local variations of functional network properties, and expand to multicenter investigations involving larger numbers of participants to examine not only age-related variations but also sex-related differences. In addition, we plan to establish an EEG-based automated algorithm to estimate brain maturity levels from early childhood to adolescence for use in the clinical diagnosis and treatment of age-related brain disorders, which has already been attempted in some previous fMRI studies.[62,63]

Conclusion

We investigated longitudinal variations of the resting-state EEG-based functional networks from early childhood to adolescence in six frequency bands using eight types of functional connectivity measures with different domain specificities of amplitude, frequency, and phase. Our conclusions are as follows: first, electrophysiological aspects of network-based pediatric brain maturation are characterized by increases in both functional segregation and integration (especially noticeably up to middle adolescence) that establish functionally specialized areas and enhance neural transmission efficiency concurrently, based on reorganization of corticocortical functional connections. Second, the age-related changes in functional network properties were more accurately reflected by EEG oscillations in the upper alpha band than by those in other frequency bands, which is presumably linked to specific roles of the upper alpha band in brain development with knowledge acquisition. Third, phase-domain measures robustly reflect significant age-related changes in the upper alpha band owing to their methodological benefits compared with amplitude- and frequency-domain measures. Fourth, the functional connectivity measures susceptible to volume-conduction effects showed significant age-related changes in functional network properties in the delta, upper alpha, alpha, and beta bands. However, their connectivity strengths were inflated by spurious or ghost connections, consequently indicating that the frequency-band-specific age-related changes are influenced more by volume-conduction effects than by the domain specificity.

Supplementary Materials

The online-only Data Supplement is available with this article at https://doi.org/10.3988/jcn.2022.18.5.581.

Availability of Data and Material

Dataset unavailable.

ORCID iDs

Yoon Gi Chung	https://orcid.org/0000-0002-2656-3317
Yonghoon Jeon	https://orcid.org/0000-0002-0024-6890
Ryeo Gyeong Kim	https://orcid.org/0000-0001-9228-823x
Anna Cho	https://orcid.org/0000-0001-7500-5955
Hunmin Kim	https://orcid.org/0000-0001-6689-3495
Hee Hwang	https://orcid.org/0000-0002-7964-1630
Jieun Choi	https://orcid.org/0000-0001-6845-8745
Ki Joong Kim	https://orcid.org/0000-0002-0849-125x

Author Contributions

Conceptualization: Hunmin Kim, Hee Hwang, Jieun Choi, Ki Joong Kim. Data curation: Yoon Gi Chung, Yonghoon Jeon, Ryeo Gyeong Kim, Anna Cho, Hunmin Kim. Formal analysis: Yoon Gi Chung, Yonghoon Jeon, Hunmin Kim. Funding acquisition: Hunmin Kim, Hee Hwang. Investigation: Yoon Gi Chung, Yonghoon Jeon, Hunmin Kim. Methodology: Yoon Gi Chung, Yonghoon Jeon, Hunmin Kim. Project administration: Hunmin Kim. Resources: Anna Cho, Hunmin Kim, Hee Hwang, Jieun Choi. Software: Yoon Gi Chung, Yonghoon Jeon. Supervision: Hunmin Kim. Validation: Yoon Gi Chung, Hunmin Kim. Visualization: Yoon Gi Chung, Yonghoon Jeon, Hunmin Kim. Writing—original draft: Yoon Gi Chung, Hunmin Kim. Writing—review & editing: Yoon Gi Chung, Hunmin Kim.

Conflicts of Interest

The authors have no potential conflicts of interest to disclose.

Funding Statement

This work was supported by the Institute for Information & Communications Technology Promotion (IITP) grant funded by the Ministry of Science and ICT (MSIT), Republic of Korea (No. 2018-0-00861, Intelligent SW Technology Development for Medical Data Analysis).

REFERENCES

1. Bullmore E, Sporns O. Complex brain networks: graph theoretical analysis of structural and functional systems. *Nat Rev Neurosci* 2009;10:186-198.
2. Sporns O, Chialvo DR, Kaiser M, Hilgetag CC. Organization, development and function of complex brain networks. *Trends Cogn Sci* 2004;8:418-425.
3. Bassett DS, Sporns O. Network neuroscience. *Nat Neurosci* 2017;20:353-364.
4. van Diessen E, Numan T, van Dellen E, van der Kooi AW, Boersma M, Hofman D, et al. Opportunities and methodological challenges in EEG and MEG resting state functional brain network research. *Clin Neurophysiol* 2015;126:1468-1481.
5. Wang HE, Bénar CG, Quilichini PP, Friston KJ, Jirsa VK, Bernard C. A systematic framework for functional connectivity measures. *Front Neurosci* 2014;8:405.
6. Smith SM, Miller KL, Salimi-Khorshidi G, Webster M, Beckmann CF, Nichols TE, et al. Network modelling methods for FMRI. *Neuroimage* 2011;54:875-891.
7. van Mierlo P, Papadopoulou M, Carrette E, Boon P, Vandenberghe S, Vonck K, et al. Functional brain connectivity from EEG in epilepsy: seizure prediction and epileptogenic focus localization. *Prog Neurobiol* 2014;121:19-35.
8. Greenblatt RE, Pflieger ME, Ossadtchi AE. Connectivity measures applied to human brain electrophysiological data. *J Neurosci Methods* 2012;207:1-16.
9. Bakhshayesh H, Fitzgibbon SP, Janani AS, Grummett TS, Pope KJ. Detecting synchrony in EEG: a comparative study of functional connectivity measures. *Comput Biol Med* 2019;105:1-15.
10. Daffertshofer A, Ton R, Kringelbach ML, Woolrich M, Deco G. Distinct criticality of phase and amplitude dynamics in the resting brain. *Neuroimage* 2018;180(Pt B):442-447.
11. Imperatori LS, Betta M, Cecchetti L, Canales-Johnson A, Ricciardi E, Siclari F, et al. EEG functional connectivity metrics wPLI and wSMI account for distinct types of brain functional interactions. *Sci Rep* 2019;9:8894.
12. Demuru M, La Cava SM, Pani SM, Fraschini M. A comparison between power spectral density and network metrics: an EEG study. *Biomed Signal Process Control* 2020;57:101760.
13. Siems M, Siegel M. Dissociated neuronal phase- and amplitude-coupling patterns in the human brain. *Neuroimage* 2020;209:116538.
14. Bastos AM, Schoffelen JM. A tutorial review of functional connectivity analysis methods and their interpretational pitfalls. *Front Syst Neurosci* 2016;9:175.
15. Palva JM, Wang SH, Palva S, Zhigalov A, Monto S, Brookes MJ, et al. Ghost interactions in MEG/EEG source space: a note of caution on inter-areal coupling measures. *Neuroimage* 2018;173:632-643.
16. Wig GS. Segregated systems of human brain networks. *Trends Cogn Sci* 2017;21:981-996.
17. Cao M, Huang H, He Y. Developmental connectomics from infancy through early childhood. *Trends Neurosci* 2017;40:494-506.
18. Stevens MC. The contributions of resting state and task-based functional connectivity studies to our understanding of adolescent brain network maturation. *Neurosci Biobehav Rev* 2016;70:13-32.
19. Fair DA, Dosenbach NU, Church JA, Cohen AL, Brahmbhatt S, Miezin FM, et al. Development of distinct control networks through segregation and integration. *Proc Natl Acad Sci U S A* 2007;104:13507-13512.
20. Fair DA, Cohen AL, Dosenbach NU, Church JA, Miezin FM, Barch DM, et al. The maturing architecture of the brain's default network. *Proc Natl Acad Sci U S A* 2008;105:4028-4032.
21. Gu S, Satterthwaite TD, Medaglia JD, Yang M, Gur RE, Gur RC, et al. Emergence of system roles in normative neurodevelopment. *Proc Natl Acad Sci U S A* 2015;112:13681-13686.
22. Kelly AM, Di Martino A, Uddin LQ, Shehzad Z, Gee DG, Reiss PT, et al. Development of anterior cingulate functional connectivity from late childhood to early adulthood. *Cereb Cortex* 2009;19:640-657.
23. Marek S, Hwang K, Foran W, Hallquist MN, Luna B. The contribution of network organization and integration to the development of cognitive control. *PLoS Biol* 2015;13:e1002328.
24. Supekar K, Musen M, Menon V. Development of large-scale functional brain networks in children. *PLoS Biol* 2009;7:e1000157.
25. Boersma M, Smit DJ, Boomsma DI, De Geus EJ, Delemarre-van de Waal HA, Stam CJ. Growing trees in child brains: graph theoretical analysis of electroencephalography-derived minimum spanning tree in 5- and 7-year-old children reflects brain maturation. *Brain Connect* 2013;3:50-60.
26. Boersma M, Smit DJ, de Bie HM, Van Baal GC, Boomsma DI, de Geus EJ, et al. Network analysis of resting state EEG in the developing young brain: structure comes with maturation. *Hum Brain Mapp* 2011;32:413-425.
27. Barry RJ, Clarke AR, McCarthy R, Selikowitz M, Johnstone SJ, Rushby JA. Age and gender effects in EEG coherence: I. Developmental trends in normal children. *Clin Neurophysiol* 2004;115:2252-2258.
28. Thatcher RW, North DM, Biver CJ. Self-organized criticality and the development of EEG phase reset. *Hum Brain Mapp* 2009;30:553-574.
29. Fraschini M, Demuru M, Crobe A, Marrosu F, Stam CJ, Hillebrand A. The effect of epoch length on estimated EEG functional connectivity and brain network organisation. *J Neural Eng* 2016;13:036015.
30. Christodoulakis M, Hadjipapas A, Papathanasiou ES, Anastasiadou M, Papacostas SS, Mitsis GD. On the effect of volume conduction on graph theoretic measures of brain networks in epilepsy. In: Sakkalis V, editor. *Modern Electroencephalographic Assessment Techniques.* New York: Springer, 2015;103-130.
31. Nevado A, Hadjipapas A, Kinsey K, Moratti S, Barnes GR, Holliday IE, et al. Estimation of functional connectivity from electromagnetic signals and the amount of empirical data required. *Neurosci Lett* 2012;513:57-61.
32. Nolte G, Bai O, Wheaton L, Mari Z, Vorbach S, Hallett M. Identifying true brain interaction from EEG data using the imaginary part of coherency. *Clin Neurophysiol* 2004;115:2292-2307.
33. Lachaux JP, Rodriguez E, Martinerie J, Varela FJ. Measuring phase synchrony in brain signals. *Hum Brain Mapp* 1999;8:194-208.
34. Bruña R, Maestú F, Pereda E. Phase locking value revisited: teaching new tricks to an old dog. *J Neural Eng* 2018;15:056011.
35. Stam CJ, Nolte G, Daffertshofer A. Phase lag index: assessment of functional connectivity from multi channel EEG and MEG with diminished bias from common sources. *Hum Brain Mapp* 2007;28:1178-1193.
36. Vinck M, Oostenveld R, van Wingerden M, Battaglia F, Pennartz CM. An improved index of phase-synchronization for electrophysiological data in the presence of volume-conduction, noise and sample-size bias. *Neuroimage* 2011;55:1548-1565.
37. Pascual-Marqui RD. Instantaneous and lagged measurements of linear and nonlinear dependence between groups of multivariate time series: frequency decomposition. arXiv [Preprint]. 2007. [cited 2021 May 14]. Available at: https://doi.org/10.48550/arXiv.0711.1455.
38. Pascual-Marqui RD. Coherence and phase synchronization: generalization to pairs of multivariate time series, and removal of zero-lag contributions. arXiv [Preprint]. 2007 [cited 2021 May 14]. Available at: https://doi. org/10.48550/arXiv.0706.1776.
39. Rubinov M, Sporns O. Complex network measures of brain connectivity: uses and interpretations. *Neuroimage* 2010;52:1059-1069.
40. Dancey CP, Reidy J. *Statistics without maths for psychology.* 4th ed. Harlow: Pearson Education Limited, 2007.
41. Benjamini Y, Yekutieli D. The control of the false discovery rate in multiple testing under dependency. *Ann Stat* 2001;29:1165-1188.
42. Delorme A, Makeig S. EEGLAB: an open source toolbox for analysis of single-trial EEG dynamics including independent component analysis. *J Neurosci Methods* 2004;134:9-21.
43. Smit DJ, Boersma M, Schnack HG, Micheloyannis S, Boomsma DI,

Hulshoff Pol HE, et al. The brain matures with stronger functional connectivity and decreased randomness of its network. *PLoS One* 2012;7:e36896.
44. Faghiri A, Stephen JM, Wang YP, Wilson TW, Calhoun VD. Changing brain connectivity dynamics: from early childhood to adulthood. *Hum Brain Mapp* 2018;39:1108-1117.
45. Ferreira LK, Busatto GF. Resting-state functional connectivity in normal brain aging. *Neurosci Biobehav Rev* 2013;37:384-400.
46. Zuo XN, Kelly C, Di Martino A, Mennes M, Margulies DS, Bangaru S, et al. Growing together and growing apart: regional and sex differences in the lifespan developmental trajectories of functional homotopy. *J Neurosci* 2010;30:15034-15043.
47. Lopez-Larson MP, Anderson JS, Ferguson MA, Yurgelun-Todd D. Local brain connectivity and associations with gender and age. *Dev Cogn Neurosci* 2011;1:187-197.
48. Gabard-Durnam LJ, Flannery J, Goff B, Gee DG, Humphreys KL, Telzer E, et al. The development of human amygdala functional connectivity at rest from 4 to 23 years: a cross-sectional study. *Neuroimage* 2014;95:193-207.
49. Ishii R, Canuet L, Aoki Y, Hata M, Iwase M, Ikeda S, et al. Healthy and pathological brain aging: from the perspective of oscillations, functional connectivity, and signal complexity. *Neuropsychobiology* 2017;75:151-161.
50. Babiloni C, Binetti G, Cassarino A, Dal Forno G, Del Percio C, Ferreri F, et al. Sources of cortical rhythms in adults during physiological aging: a multicentric EEG study. *Hum Brain Mapp* 2006;27:162-172.
51. Nobukawa S, Kikuchi M, Takahashi T. Changes in functional connectivity dynamics with aging: a dynamical phase synchronization approach. *Neuroimage* 2019;188:357-368.
52. Klimesch W. EEG alpha and theta oscillations reflect cognitive and memory performance: a review and analysis. *Brain Res Brain Res Rev* 1999;29:169-195.
53. Robertson EK, Köhler S. Insights from child development on the relationship between episodic and semantic memory. *Neuropsychologia* 2007;45:3178-3189.
54. Thatcher RW. Cyclic cortical reorganization during early childhood. *Brain Cogn* 1992;20:24-50.
55. Guevara R, Velazquez JL, Nenadovic V, Wennberg R, Senjanovic G, Dominguez LG. Phase synchronization measurements using electroencephalographic recordings: what can we really say about neuronal synchrony? *Neuroinformatics* 2005;3:301-314.
56. Briels CT, Schoonhoven DN, Stam CJ, de Waal H, Scheltens P, Gouw AA. Reproducibility of EEG functional connectivity in Alzheimer's disease. *Alzheimers Res Ther* 2020;12:68.
57. Sakkalis V, Doru Giurc Neanu C, Xanthopoulos P, Zervakis ME, Tsiaras V, Yang Y, et al. Assessment of linear and nonlinear synchronization measures for analyzing EEG in a mild epileptic paradigm. *IEEE Trans Inf Technol Biomed* 2009;13:433-441.
58. Dauwels J, Vialatte F, Musha T, Cichocki A. A comparative study of synchrony measures for the early diagnosis of Alzheimer's disease based on EEG. *Neuroimage* 2010;49:668-693.
59. Silfverhuth MJ, Hintsala H, Kortelainen J, Seppänen T. Experimental comparison of connectivity measures with simulated EEG signals. *Med Biol Eng Comput* 2012;50:683-688.
60. Mezeiová K, Paluš M. Comparison of coherence and phase synchronization of the human sleep electroencephalogram. *Clin Neurophysiol* 2012;123:1821-1830.
61. Ruiz-Gómez SJ, Hornero R, Poza J, Maturana-Candelas A, Pinto N, Gómez C. Computational modeling of the effects of EEG volume conduction on functional connectivity metrics. Application to Alzheimer's disease continuum. *J Neural Eng* 2019;16:066019.
62. Dosenbach NU, Nardos B, Cohen AL, Fair DA, Power JD, Church JA, et al. Prediction of individual brain maturity using fMRI. *Science* 2010;329:1358-1361.
63. Satterthwaite TD, Wolf DH, Ruparel K, Erus G, Elliott MA, Eickhoff SB, et al. Heterogeneous impact of motion on fundamental patterns of developmental changes in functional connectivity during youth. *Neuroimage* 2013;83:45-57.